Fluid Dynamics and Aerodynamics Program

Sibley School of
Mechanical and Aerospace Engineering

Cornell University Ithaca, New York 14853

Prediction of the Turbulent Wake with Second-Order Closure*

by

D. B. Taulbee and J. L. Lumley

FDA-81-04 May 1981

*Supported in part by the U.S. National Science Foundation under Grants No. ATM 79-22006 and CME 79-19817, in part by the U.S. Office of Naval Research under the following programs: Fluid Dynamics (Code 438), Power (Code 473) and Physical Oceanography (Code 481), and in part by the U.S. NASA-Ames Research Center under GRant No. NSG-2382.

**Department of Mechanical and Aerospace Engineering, State University of New York at Buffalo, NY.

***Sibley School of Mechanical and Aerosoace Engineerng, Cornell University, Ithaca, NY.

Introduction

Since approximately 1968 there has been an explosive development of second-order modeling of turbulence (also called invariant modeling or one-point closure). This is described in detail in Lumley (1978), and in several other survey articles. Briefly, equations are carried for the various second order quantities (the variances and the fluxes), and the unknown terms appearing in these equations are modeled as functions of the second order quantities, so as to obtain a closed system.

The approach has been remarkably successful. This is probably because more of the physical mechanisms are carried exactly (unmodeled) in the second order equations. Of course, constants are included which are adjusted by calibration of the model against benchmark situations. If the second-order models are applied in a situation in which a first-order (mixing length) model is adequate, the second-order model usually is not an improvement. Probably here the additional mechanisms carried exactly are of minor importance (or the first-order model would not work), and the crudeness of the various closures adopted probably negates the slight additional accuracy. The second-order models will, however, deal with many situations in which the first-order models do not work at all (because of the presence of the additional mechanisms).

There are still many ways in which these closures are not adequate, however. The constants are by no means universal. In some situations it is clear that a physical mechanism has been omitted - for example, two-dimensional and axisymmetric jet flows cannot be predicted with the same

constants (Launder & Mor , 1979). The effect of swirl has not been included (Lumley, 1981). The closures generally used do not guarantee realizability; that is, they do not guarantee that quantities that should be non-negative will remain so, or that correlation coefficients will remain less than unity in absolute value.

We feel that some of these problems can be alleviated by a more formal approach to the development of these closures. Although certain of the concepts of Rational Mechanics have been used from the beginning, they have not been applied as extensively or consistently as they could have been. Realizability has not been extensively used to develop closure forms. Many closures are essentially ad hoc, and are not tied to a physical model. If closures were developed from specific physical models, it should be possible to obtain the values of the constants from these models, rather than calibrating the models against benchmark flows.

Lumley (1978) attempted to implement these ideas. In many ways the closure presented there is not markedly different from those in common use. Some of the forms were minor improvements; in other cases it was clear what was wrong with the forms in common use, but it was not clear how to devise an improvement. In one respect, however, the closure presented in Lumley (1978) was markedly different: the third moments (the fluxes of the variances and fluxes) were obtained from an orderly perturbation procedure about a Gaussian equilibrium state. The third moment equations thus obtained were minor variations on those suggested on an ad hoc basis by Hanjalic & Launder (1972), with one important difference: no additional adjustable constants were introduced. Thus, the transport of fluxes and variances cannot be separately adjusted in a calculation.

Briefly, a turbulence was envisioned whose energy containing scales would be Gaussian in the absence of inhomogeneity, gravity, etc. An equation was constructed for a function equivalent to the probability density, the second moment of which corresponded to the accepted modeled form of the Reynolds stress equation. The third moment equations obtained from this (which were thus guaranteed to be consistent) were simplified by the assumption of weak inhomogeneity.

The purpose of this paper is to present calculations with this model, and interpretations of the results. In the following section we give an outline of the model. The details of the development are given in Lumley (-1978).

2. The Model

The dynamic equation for Reynolds stress in an isothermal turbulent flow can be written

$$\begin{aligned}\dot{\overline{u_i u_j}} + (\overline{u_i u_j})_{,k} U_k = &- (U_{i,k}\overline{u_k u_j} + U_{j,k}\overline{u_k u_i}) \\ &- \{\overline{u_i u_j u_k} + \overline{p u_j}\delta_{ik}/\rho + \overline{p u_i}\delta_{jk}/\rho\}_{,k} \\ &+ [\overline{p^{(2)}(u_{i,j} + u_{j,i})/\rho} - 2\nu\overline{u_{i,k}u_{j,k}} + 2\bar{\epsilon}\delta_{ij}/3] \\ &+ \overline{p^{(1)}(u_{i,j} + u_{j,i})/\rho} - 2\bar{\epsilon}\delta_{ij}/3\end{aligned} \tag{1}$$

which states that the substantial change of $\overline{u_i u_j}$ during convection is equal to the production of Reynolds stress from the mean flow plus the divergence of the flux of Reynolds Stress and pressure due to turbulent fluctuations plus the return toward isotropy of the Reynolds stress tensor, plus the "rapid" change of $\overline{u_i u_j}$, plus the (isotropic) dissipation of $\overline{u_i u_j}$ into heat, respectively. The quantity $\bar{\epsilon}$ is the total dissipation. At large Reynolds numbers turbulence at the scales at which dissipation occurs becomes isotropic, hence, $2\nu\overline{u_{i,k}u_{j,k}} \to 2\bar{\epsilon}\delta_{ij}/3$ in equation 1. The pressure-strain correlation has been divided into two parts, associated respectively with the two Poisson equations

$$-p^{(1)}_{,ii}/\rho = 2U_{i,j}u_{j,i} \tag{2}$$

$$-p^{(2)}_{,ii}/\rho = u_{i,j}u_{j,i} - (\overline{u_i u_j})_{,ij} \tag{3}$$

where the first is related to the mean velocity gradient and is linear in the fluctuating velocity, while the second is quadratic in the fluctuating components. The second is responsible for the return of anisotropic turbulence toward isotropy.

The quantity in the square brackets in equation (1) is a symmetric tensor with zero trace, and vanishes if the turbulence is isotropic. Since this term acts to interchange energy among the components when the turbulence is anisotropic it is natural to express it in terms of the anisotropy tensor of the Reynolds stress

$$b_{ij} = \overline{u_i u_j}/\bar{q}^2 - \delta_{ij}/3 \qquad (4)$$

giving

$$\overline{\gamma^{(2)}(u_{i,j} + u_{j,i})/\rho} - 2\nu\overline{u_{i,k}u_{j,k}} + 2\bar{\epsilon}\delta_{ij}/3 = -C_1\bar{\epsilon}b_{ij} \qquad (5)$$

where the inclusion of $\bar{\epsilon}$ makes the expression dimensionally correct. The coefficient C_1 can depend on the Reynolds number and the invariants of the anisotropy tensor, since C_1 must itself be an invariant. Hence.

$$C_1 = C_1(II, III, R_\ell) \qquad (6)$$

where $II = -b_{ij}b_{ji}/2$, $III = b_{ij}b_{jk}b_{ki}/3$

and $R_\ell = (\bar{q}^2)^2/9\bar{\epsilon}\nu$. If any one of the velocity components vanishes or if Schwarz's inequality between any two components is on the verge of being violated, it can be shown that $C_1 \to 2$. Hence, to ensure realizability, that non-negative quantities, such as the component intensities, remain positive and Schwarz's inequality is satisfied we must have $C_1 \geq 2$. Furthermore it can be shown that

$$1/9 + 3III + II \geq 0 \qquad (7)$$

and is zero only when one eigenvalue of $\overline{u_i u_j}$ vanishes. Both the vanishing of a component and the violation of Scharz's inequality are equivalent to the vanishing of an eigenvalue. These considerations suggest that C_1 is of the form

$$C_1 = 2 + (1/9 + 3III + II)\,F(II, III, R_\ell) \qquad (8)$$

The function F must reflect the trend that $C_1 \to 2$ as $Re \to 0$ and $C_1 \to 2$ as $Re \to \infty$ as indicated by the data of Comte-Bellot & Corrsin (1966). A function that satifies these conditions and fits the data of Uberoi (see Lumley & Newman 1977) in the mid range of anisotropy is

$$F = \exp\left[-7.77/R_e^{1/2}\right]\left\{72/R_e^{1/2} + 80.1\ln\left[1 + 62.4(-\Pi + 1.3)\right]\right\} \quad (9)$$

The condition of realizability is then satisfied with the form of C_1 given by equations (8) and (9).

The rapid term $\overline{p^{(1)}(u_{i,j} + u_{j,i})/\rho}$ has zero trace and, therefore, redistributes energy among the component intensities. Using the Fourier transform solution of equation (2), assuming a homogeneous mean field, the rapid term becomes

$$\overline{p^{(1)}(u_{i,j} + u_{j,i})/\rho} = 2\,U_{p,q}\left(I_{piqj} + I_{pjqi}\right)\overline{q^2} \quad (10)$$

where

$$I_{piqj} = \int (\kappa_i \kappa / \kappa^2)\, S_{qj}\, d\underline{\kappa} \quad (11)$$

and S_{qj} is the spectrum of the Reynolds stress. From equation (10) it is apparent that the rapid term arises from the interaction of the turbulence with mean flow velocity gradients. The fourth order tensor must satisfy

$$I_{piqj} = I_{pijq} \quad ; \quad I_{piqj} = I_{ipqj}$$

for symmetry, $I_{piij}=0$ for incompressibility,

$$I_{pqqj} = \overline{u_q u_j}/\overline{q^2}$$

and when the turbulence is isotropic

$$I_{iqqj} = (4\,\delta_{ij}\delta_{pq} - \delta_{pi}\delta_{qj} - \delta_{pj}\delta_{qi})/3$$

which can be determined directly from equation (11) since the form of the spectrum for isotropic turbulence is known. In general this tensor would at least depend on the anisotropy tensor and the Reynolds number. We take the

tensor to be linear in the anisotropy tensor. A form which satisfies all the above requirements is

$$I_{pi,qj} = (4\delta_{pi}\delta_{qj} - \delta_{pq}\delta_{ij} - \delta_{pj}\delta_{qi})/30 - (b_{pi}\delta_{qj} - \delta_{pi}b_{qj})/3 + C[b_{pq}\delta_{ij} + b_{iq}\delta_{pj} + b_{pj}\delta_{iq} + b_{ij}\delta_{pq} - 11\, b_{pi}\delta_{qj}/3 - 7\,\delta_{pi}b_{qj}/3] \quad (12)$$

There is no information on the variation with Reynolds number and we will take C to be a fixed constant.

The constant C has somewhat different values when evaluated for different flows. Reynolds (1976) found C = -0.1 works better for the experiment of Tucker & Reynolds (1968) and C = -0.2 works better for the flow of Champagne, Harris & Corrsin (1978). Reynolds recommends C = -0.15. Launder, Reece & Rodi (1975) use a value of -0.145, which they base on homogeneous experiments. Lumley (1978b) suggests C = -0.166 to give a reasonable agreement with experimental data. In the present calculations we use C = -0.15. We note that increasing or decreasing C by 10 percent produced only slight variations in the results for the wake; if, by changing C, better results for the component energies were obtained, then poorer results in comparison with experimental data were obtained for the shear stress.

By formulating a dynamic equation for the cumulant C_{ijk} (corresponding to the triple velocity correlation) and performing an order-of-magnitude analysis for the case of weak inhomogeneity (homogeneous turbulence is observed to be approximately Gaussian in the energy containing eddies and departure from Gaussian behavior is associated with inhomogeneity, that is, non-zero values of $\overline{u_iu_ju_k}$ are fluxes and are necessarily non-Gaussian) it can be shown (see Lumley 1978a)

$$\overline{u_iu_ju_k} = -\frac{1}{3C_1}\frac{\bar{q}^2}{\bar{\epsilon}}\left[G_{ijk} + \frac{C_1-2}{4C_1+10}(\delta_{ij}G_k + \delta_{ik}G_j + \delta_{jk}G_i)\right] \quad (13)$$

$$\overline{q^2u_i} = \frac{3}{4C_1+10}\cdot\frac{\bar{q}^2}{\bar{\epsilon}}G_i \quad (14)$$

where

$$G_{ijk} = \overline{u_k u_p}\,(\overline{u_i u_j})_{,p} + \overline{u_j u_p}\,(\overline{u_i u_k})_{,p} + \overline{u_i u_p}\,(\overline{u_j u_k})_{,p}$$

$$G_k = \overline{u_k u_l}\;\overline{q^2}_{,l} + 2\,\overline{u_q u_l}\,(\overline{u_q u_k})_{,l}$$

The quantity C_1 is the same coefficient given by equation (8) for the return to isotropy.

For the pressure transport, $(\overline{pu_j}_{,i} + \overline{pu_i}_{,j})/\rho$, we begin from equation (3) for the second (return to isotropy) part of the pressure for a homogeneous flow and obtain by use of Fourier transforms

$$-\overline{p^{(1)}u_k}/\rho = \int (\kappa_i \kappa_j/\kappa^2)\, S_{ijk}\, d\underline{\kappa} \qquad (15)$$

where S_{ijk} is the spectrum of $\overline{u_i u_j u_k}$.

Defining

$$I_{ijpq} = \int (\kappa_i \kappa_j/\kappa^2)\, S_{pqr}\, d\underline{\kappa} \qquad (16)$$

we have $I_{ijpq} = I_{jipq}$ and $I_{ijpq} = I_{ijqp}$ from symmetry, $I_{ijpq}\kappa_j = 0$ from incompressibility, and $I_{iipq} = \overline{u_p u_q u_r}$. The most general linear form for I_{ijpq} contains five coefficients; however, applying the various conditions, we can determine them all:

$$I_{ijpq} = 2\delta_{ij}\,\overline{u_p u_q u_r}/5 - (\delta_{ip}\,\overline{u_j u_p u_q} + \delta_{jp}\,\overline{u_i u_p u_q})/10 \qquad (17)$$

then

$$-\overline{p^{(2)}u_r}/\rho = I_{ijij} = \overline{q^2 u_r}/5 \qquad (18)$$

where $\overline{q^2 u_r}$ is given by equation (14). If $u_r \to 0$, the expression vanishes, and realizability is satisfied.

To complete the set of equations the dissipation must be calculated. For this we use a convection-transport equation with a production

/destruction term

$$\dot{\bar{\epsilon}} + \bar{\epsilon}_{,i}\bar{U}_i + (\bar{\epsilon}\bar{u}_i)_{,i} = -(\bar{\epsilon}^2/\bar{q}^2)\psi \tag{19}$$

where ψ is a dimensionless invariant function. It is reasonable to assume that ψ depends on the Reynolds stress, the mean velocity gradient, the dissipation and the viscosity. Hence,

$$\psi = \psi(b_{ij}, \bar{q}^2\bar{U}_{i,j}/\bar{\epsilon}, Re) \tag{20}$$

This must now be a function of the invariants that can be constructed from these quantities. We make the stipulation that the mean velocity gradient does not appear without the anisotropy, because we do not expect to change the level of the dissipation by a change in the mean gradient if the turbulence is isotropic. There are a large number of invariants that can be formed between the mean velocity gradient and the anisotrppy and we only give a few:

$$\psi = \psi(II, III, b_{ij}\bar{q}^2\bar{U}_{i,j}/\bar{\epsilon}, b^2_{ij}\bar{q}^2\bar{U}_{i,j}/\bar{\epsilon}, \ldots, Re) \tag{21}$$

Assuming the velocity gradient to be small we can expand this function in a power series

$$\psi = \psi_0 + \psi_1 b_{ij}\bar{q}^2\bar{U}_{i,j}/\bar{\epsilon} + \psi_2 b^2_{ij}\bar{q}^2\bar{U}_{i,j}/\bar{\epsilon} + \cdots \tag{22}$$

where the coefficients are functions of the invariants of the anisotropy tensor and Reynolds numbers.

The coefficients in the above expression must be determined from experimental data. Lumley and Newman (1977) found that $\psi_0 = 14/5$ for two limiting cases with no production from mean velocity gradients: the final period of decay for small Reynolds numbers and for one-dimensional turbulence. With these considerations the following formula approximates the data of Comte-Bellot & Corrsin (1966)

$$\psi_0 = 14/5 + 0.980\ \exp\left[-2.43\, Re^{-1/2}\right]\left[1 - 0.337 \ln(1 + 55\Pi)\right] \qquad (23)$$

For the production term we use the value $\psi_1 = 2.0$ as given by Reynolds as was determined from the nearly homogeneous shear flows of Tucker & Reynolds (1968) and Champagne, Harris & Corrsin (1966). Assuming the anisotropy to be not too large we ignore the ψ_2-term in equation (22).

To determine the transport flux $\overline{\epsilon u_k}$ for dissipation we note that the eddy viscosity $(\overline{q^2})^2/\bar{\epsilon}$ does not vary greatly across much of the width of free shear flows. Also $(\overline{q^2})^{m}/\bar{\epsilon}$ must remain finite as both $\bar{\epsilon}$ and $\overline{q^2}$ vanish (e.g.- at the edge of a wake or jet.) Presuming that $(\overline{q^2})^{m}/\bar{\epsilon} \sim$ constant we have

$$\overline{q^2}\,\bar{\epsilon}_{,k} = m\,\bar{\epsilon}\,\overline{q^2}_{,k} \qquad (24)$$

Drawing an analogy from this relation we can write for the transport

$$\overline{q^2}\,(\overline{\epsilon u_k})_{,k} = m\,\bar{\epsilon}\left[\overline{(q^2 + 2p/\rho)u_k}\right]_{,k} \qquad (25)$$

where we have included pressure transport in the total transport. This relation stipulates that as the energy transport vanishes so must the dissipation transport. Using equation (18) for the pressure transport we obtain

$$\overline{\epsilon u_k} = (3m\,\bar{\epsilon}/5\overline{q^2})\,\overline{q^2 u_k} \qquad (26)$$

Using equation (14) for $\overline{q^2 u_k}$, but replacing

$$(\overline{u_i u_j})_{,k} = (\overline{u_i u_j}/m\bar{\epsilon})\,\bar{\epsilon}_{,k} \qquad (27)$$

we obtain for the dissipation transport flux

$$\overline{\epsilon u_k} = \left[-0.9/(2C_1 + 5)\right](\overline{q^2}/\bar{\epsilon})\left[\overline{u_k u_p} + 2\,\overline{u_k u_k}\,\overline{u_j u_i}/\overline{q^2}\right]\bar{\epsilon}_{,p} \qquad (28)$$

Although obtained on somewhat tenuous grounds this result gives about the right magnitude for the dissipation transport flux and it has the advantage that no new constants are introduced.

2. Calculation of the Wake

The isothermal far-wake downstream of an object in an initially uniform flow provides a relatively simple yet comprehensive testing ground for a turbulence model. The simplification arises from the fact that some distance downstream of the object the velocity defect is small and the convective term can linearized. However, all possible ingredients for an isothermal turbulent flow are present; convection, mean velocity gradients, anisotropy, production, and redistribution due to rapid terms and transport.

In terms of the dimensioness velocity defect $U = (U_{1,\infty} - U_1)/U_{1,\infty}$ and dimensionless coordinates $x = x_1/\theta$, $y = x_2/\theta$ where θ is the momentum thickness of the wake. the component equations for the two-dimensional wake are given in Appendix 1 and those for the axisymmetric wake in Appendix 2. The only mean flow component of significance is U and except for the convection terms all gradients in the flow direction can be neglected.

Since the equations are parabolic in the x-direction and boundary valued in the y-direction we can solve them by marching in the x-direction from an initial station, solving a boundary value problem in the y-direction at each x-location. A simple implicit scheme was formulated, using a simple backward difference in the x-direction with central differences in the y-direction. At each x-position the equations for the Reynolds stresses are solved sequentially. The diffusion term in the variable in question, along with part of the return-to-isotropy and convection terms, are treated implicitly. The other diffusion terms, production, rapid terms, etc. are treated explicitly and are evaluated at the upstream station. Finite differencing the implicit terms gives a set of algebraic equations whose coefficient matrix is tridiagonal and which is readily solved by an elimination procedure. After the Reynolds stresses are computed the dissipation equation is solved in a similar manner. Then the mean velocity defect U is determined from the momentum equation.

The boundary conditions at the centerline are symmetry conditions on all the variables except for $\overline{uv}$ whose value is zero there. At the outer edge

all variables approach zero. However, since some terms in the equations contain $\overline{q^2}$ or $\bar{\epsilon}$ in the denominator. it is necessary to add a small number, taken as a small fraction of the center values, to $\overline{q^2}$ and $\bar{\epsilon}$ in order to avoid dividing by zero in the calculations. The outer edge was taken at $y_\ell = 4\ell$ where ℓ is the position where $U/U_\ell = \exp(-.5)$. For the first station 50 intervals were taken across half the wake. As the wake grows more intervals are added corresponding to $y_\ell = 4\ell$ until there are 100, at which point y is doubled and every other point is retained so that there are again 50 intervals.

Since we are interested in obtaining the far field self-preserving wake, the initial conditions specified at x = 1, were chosen somewhat arbitrarily. The similarity solution with constant eddy viscosity given in Tennekes & Lumley (1972) was used for the velocity profile, $U/U_\ell = \exp(-0.5\ y^2/\ell^2)$, where $U_\ell = 1.44\ x^{-1/2}$ and $\ell = 0.277\ x^{1/2}$ for a circular cylinder and $U_\ell = 0.575\ x^{-2/3}$ and $\ell = 0.452\ x^{1/3}$ for a sphere. The key input parameter is the value of the momentum integral which is $\int_{-\infty}^{+\infty} U dy = 1$ for two dimensions and $\int_0^\infty Urdr = 1/8$ for the axisymmetric wake. The values of these integrals were continuously monitored in the calculations to ensure their constancy. The initial shear stress profile $\overline{uv}$ was also determined from the eddy viscosity solution. The turbulent velocity is given by $\overline{q^2} \cong -7.5\ \overline{uv}$ and the dissipation is roughly the production for $y \geq \ell$, Tennekes & Lumley (1972). For $0 \leq y \leq \ell$, $\overline{q^2}$ and $\bar{\epsilon}$ are taken equal to the values at $y = \ell$. The component energies were taken to be one third of the total turbulent energy.

For the two-dimensional case the results are presented for x = 1000, after 500 steps, where the profiles are self preserving when scaled by U_ℓ and ℓ. Scaled results at x = 2000 were less than a few percent different than those at x = 1000. Changes in the initial conditions produced little difference in the self-preserving behavior of the solutions. Results for the axisymmetric case are presented for x = 500, after 500 steps. A numerical instability occurred around x = 700 in attempts to compute to larger distances. Even so, the profiles were nearly self-preserving at x = 500.

Results and Discussion

The calculated predictions for the mean velocities and Reynolds stresses are compared with experimental results of Chevray & Kovasznay 1969 (for the wake behind a flat plate) and Townsend 1956 (for the wake behind a circular cylinder) in Figures 1-5. Overall the agreement between predictions and the flat-plate experimental results are quite good. The data for $\overline{v^2}/U_\ell^2$ and $\overline{uv}/U_\ell^2$ for the cylinder are quite different from the predictions. We will present below our explanation for the discrepancy between the cylinder data and the calculated results. We include the cylinder both to contrast the behavior of wakes behind different objects and to indicate the trends of certain turbulent quantities that have only been measured for a cylinder. It is seen that the calculated mean velocity profiles are somewhat flatter than those measured for the flat plate wake, and the calculated shear profile is slightly lower than the measured. For self preservation these quantities are directly related by

$$\overline{uv}/U_\ell^2 = -(y/\ell)(U/U_\ell) \tag{29}$$

Probably there is a little too much diffusion in the dynamic equation for the Reynolds stress, thus giving too small a peak in the shear profile and a flatter velocity profile. We note that Townsend's shear data does not obey the self preserving relation (29).

Figure 6 shows the calculated transport flux profiles $\overline{u^2v}/U_\ell^3$, $\overline{v^3}/U_\ell^3$ and $\overline{w^2v}/U_\ell^3$ as compared to the measurements of Townsend. Although, as we shall argue below, the predictions should not compare well with the cylinder wake, the trends compare reasonably and the magnitudes are about right.

Table 1 gives the overall characteristics of the plane wake. It is seen that there is good agreement between the predicted wake growth and centerline velocity decay and the flat plate wake data. We suggest that this is so because the flat plate wake is created rather smoothly from the trailing edge boundary layers on the top and bottom of the thin plate, without vortex shedding. These conditions seem to us to be a better match to the theory, which does not specifically include transport by large eddy structures.

The cylinder, on the other hand, has alternate vortex shedding. As the flow ages these vortices lose their identity to a certain extent, but a distinct large-scale structure remains. It is generally accepted that far downstream, where the flow is in dynamic equilibrium, the wake becomes independent of everything except the initial momentum thickness. However, this universal equilibrium wake has not been observed experimentally, perhaps because measurements have not been carried out to large enough distances. What have been observed experimentally (Bevilaqua & Lykoudis 1978) are apparently self-preserving wakes, which obey the similarity laws within experimental error over the range of observation, but which are different for different objects, e.g., cylinder versus flat plate. This apparently self-preserving mode persists with seemingly little change for considerable distances, as is evidenced by Townsend's cylinder measurements which exhibit the same behavior to $x/d > 1000$. It seems possible that the effects of the near-field large scale structure (characterized by meandering of the entire wake, with strong intermittency, and the occasional appearance of non-turbulent flow on the centerline) persist to great distances, the wake

continuing to evolve, but so slowly as to be undetectable over the range of observation. It is also possible that the flat plate wake will slowly evolve its own large scale structure far downstream. This could explain the differences between the plate and cylinder wakes: the plate having little or no near-field large-scale structure quickly attains an apparent equilibrium similarity mode (from which it may be slowly evolving toward a universal state) whereas the cylinder quickly attains a different apparently self-preserving mode, which may also be slowly evolving toward a universal state; the two will not reach their common universal state until far beyond the experimental range.

It was stated in the description of the numerical procedures that the initial conditions on centerline velocity and characteristic wake dimension were chosen consistent with the measurements for the cylinder given in Table 1. Yet shortly into the the calculations, the wake characteristics tended toward the asymptotic calculated values which are close to those given for the flat plate wake. In order that the calculated constants given in Table 1 be determined independent of x_0 we used $B = 2l(dl/dx)^{1/2}$ and $A = (-U_\ell^3/(2dU_\ell/dx))^{1/2}$, which corresponds to the relations $l = B(x-x_0)^{1/2}$ and $U_\ell = A(x-x_0)^{-1/2}$ respectively. These constants closely assumed their asympototic values around $x = 100$. Furthermore, changes in initial conditions, energy, dissipation levels, etc., (except for the initial momentum thickness) had little effect on the ultimate self-preserving state, affecting only the rate at which it was attained. Despite such changes, the results tended to seek a unique self-preserving state, which we may speculate is the universal similarity equilibrium state without large scale structure.

Calculations carried out with the model of Launder, Reece, & Rodi (1975) also produced good results for the self-preserving profiles when compared to

the experimental results of Chevray & Kovasznay. In their model $C_1 = 3.25$, $C_D = 0.055$ for the diffusion coefficient in the dynamic equations for the Reynolds stresses, $C = -0.0145$, $C_\epsilon = 0.075$ for the diffusion function in the dissipation equation, $\psi_0 = 3.8$ and $\psi_1 = 2.88$. The closure formulations are those given by those authors. We found good results for the centerline velocity variation and the growth rate of the characteristic lateral dimension. However, in Hanjalic & Launder (1980) it is stated that there is no explanation why the theory predicts a growth rate which is 35% less than measured. These authors have contrasted their predictions with measurements for the circular cylinder.

Rodi (1975) organized data from ten wake studies: six circular cylinders, one normal plate, two airfoils and one aligned plate. Although there are some differences, most of these studies show consistent results for the growth constant. Rodi points out that the Chevray & Kovasznay flat plate experiment was not fully-developed in the distance in which they took measurements. It is true that the scaled turbulent intensity and shear were still changing, although the mean velocity appears to have reached self-preservation (the mean velocity field usually reaches self-preservation well before the mean turbulence field does). However, we feel that the wake of Chevray & Kosvasznay is closer to some sort of (at least temporary) equilibrium than it is to the cylinder wake, to which it does not appear to be tending.

The form of the equations for the axisymmetric wake are much the same as those for the plane wake except that the diffusion-transport terms are much more complicated. These terms have been worked out and are presented in Appendix II. Results for the round wake, calculated by procedures explained for the plane wake, are presented in Figures (7-11). Figure 7 shows excellent agreement for the mean velocity between the calculated results and

the measurements of Bevilaqua & Lykoudis (1978), for the wake downstream of a porous disk 2.54 cm in diameter (normal to the stream) and of Chevray (1969) for the wake downstream of a 6 x 1 prolate spheroid with a length Reynolds number of 2.75×10^6 (so that the boundary layer on the surface of the spheroid was turbulent). Both of these wakes were relatively smooth in the near field with no evidence of vortex shedding or large scale eddy structure from flow-visualization experiments. Hence, we hypothesize these wakes would quickly attain an apparent equilibrium similarity. The agreement between the measured and calculated normal Reynolds stress is also fair. However, comparisons for $\overline{v^2}/U_\ell^2$, $\overline{w^2}/U_\ell^2$ and $\overline{uv}/U_\ell^2$ for Chevray's spheroid shown in Figures 9-11 are not so good. The reason for this is probably that the measurements were taken at x/d = 18, a position not far enough downstream for the turbulence quantities to become self-preserving.

Table 2 gives the overall characteristics for the various wakes. It is seen that the calculated wake is close to the porous disk in centerline velocity decay and growth rate where measurements were carried out to a distance of x/d = 100. The calculated growth and centerline velocity decay is also not too different from those for the spheroid wake. Note that the behavior of the wake behind a sphere is quite different from the others: the vortex shedding, meandering of the wake and large scale structure appears to leave a significant influence on the downstream wake behavior. The difference in wakes and the possible existence of different states of self preservation is the subject of the paper by Bevilaqua & Lykoudis. We only argue here that for proper comparisons between experiment and this theory (without large scale structure) the experiments must also lack large-scale structure.

As a closing point we must mention the discrepancy that has existed over the years in predicting round and plane jets with turbulence models. A

theory with a set of constants that worked well for the plane case did a poor job of predicting the round jet. We did not find a large discrepancy for the wake when the calculations were referred to the experiments lacking in large-scale structure. Possibly our more general formulation of the return-to-isotropy coefficient, the transport terms, the pressure transport, etc., has lead to a more nearly universal theory capable of handling plane and three-dimensional flows in the absence of large-scale structure.

For the treatment of flows containing large-scale structures (presumably the majority of flows important in technology and nature) it will probably be necessary to introduce the structure explicitly by some form of stability analysis. One of us (JLL) has recently made suggestions along these lines (Lumley, 1981).

REFERENCES

Bevilaqua, P. M. & Lykoudis, P. S. 1978. Turbulence memory in self-preserving wakes. J. Fluid Mech. 89: 599-606.

Champagne, F. H., Harris, V. G. & Corrsin, S. 1970. Experiments on nearly homogeneous turbulent shear flow. J. Fluid Mech. 41: 91-139.

Chevray, R. 1968. The turblent wake of a body of revolution. ASME J. Basic Engr. 90: 275-294.

Chevray, R. & Kovasznay, L. S. G. 1969. Turbulence measurements in the wake of a thin flat plate. AIAA J. 7: 1641-1642.

Comte-Bellot, G. & Corrsin, S. 1966. The use of a contraction to improve the isotropy of grid-generated turbulence. J. Fluid Mech. 25: 657-692.

Hanjalic, K. & Launder, B. E. 1976. Contribution towards a Reynolds-stress closure for low-Reynolds-number turbulence. J. Fluid Mech., 74: 593-610.

Hanjalic, K. & Launder, B. E. 1980. Sensitizing the dissipation equation to irrotational strains. ASME J. Fluids Engr. 102: 34-40.

Launder, B. E., Reece, G. T. & Rodi, W. 1975. Progress in the development of a Reynolds stress closure. J. Fluid Mech. 68: 537-566.

Launder, B. E. & Morse, A. 1979. Numerical prediction of axisymmetric free shear flows with a second order Reynolds stress closure. In Turbulent Shear Flows I, eds. F. Durst, B. F. Launder, F. M. Schmidt and J. H. Whitelaw. Berlin/Heidelberg: Springer-Verlag.

Lumley, J. L. & Khajek-Nouri, B. 1974. Computational modeling of turbulent transport. Advances in Geophysics, 18, eds. H. E. Landsberg & J. Van Mieghem, pp. 169-192. New York: Academic Press.

Lumley, J. L. & Newman, G. 1977. The return to isotropy of homogeneous turbulence. J. Fluid Mech. 82: 161-178.

Lumley, J. L. 1978a. Computational modeling of turbulent flows. In Adv. in Appl. Mech. 18, ed. C. S. Yih, pp. 123-176. New york: Academic Press.

Lumley, J. L. 1978b. Second order modeling of turbulent flows. In Prediction Methods for Turbulent Flows, ed.: W. Kollmann, pp. 1-32. Washington, DC: Hemisphere.

Lumley, J. L. 1981a. Parameterization of Turbulent Transport in Swirling Flows. Sibley School of Mechanical and Aerospace Engineering Report No. FDA-81-02. Ithaca, NY: Cornell.

Lumley, J. L. 1981b. Coherent structures in turbulence. Transition and Turbulence, ed. R. Meyer. Madison WI: Math. Research Center (in press).

Reynolds, W. C. 1976. Computation of turbulent flows. In Annual Reviews of Fluid Mech. 8, eds. M. Van Dyke, J. V. Wehausen and J. L. Lumley, pp. 183-208. Palo Alto, CA: Annual Reviews Inc.

Rodi, J. 1975. Studies in convection 1. New York: Academic Press.

Tennekes, H. & Lumley, J. L. 1972. A First Course in Turbulence. Cambridge, MA: M.I.T. Press.

Townsend, A. A. 1956. The structure of turbulent shear flow. Cambridge, UK: University Press.

Tucker, M. J. & Reynolds, A. J. 1968. The distortion of turbulence by irrotational plane strain. J. Fluid Mech. 32: 657-673.

Appendix I

The equations for calculating the plane wake are presented here. They are written in terms of the mean flow velocity defect $U = (U_{1\infty} - U_1)/U_{1\infty}$; the non-dimensional coordinates $x = x_1/\theta$ and $y = y_1/\theta$, where x_1 is in the mean flow direction and y_1 is measured across the shear layer; and the non-dimensional turbulent velocity components $u = u_1/U_{1\infty}$, $v = u_2/U_{1\infty}$, and $w = u_3/U_{1\infty}$. The usual boundary layer assumptions and wake simplifications are employed.

Momentum equation:

$$\frac{\partial U}{\partial x} = \frac{\partial \overline{uv}}{\partial y}$$

Reynolds stress equations:

$$\frac{\partial \overline{u^2}}{\partial x} = 2\overline{uv}\frac{\partial U}{\partial y} + \frac{\partial}{\partial y}\left\{C_0 \frac{\overline{q^2}}{\epsilon}\left[(C_2+1)\overline{v^2}\frac{\partial \overline{u^2}}{\partial y} + 3C_2\overline{v^2}\frac{\partial \overline{v^2}}{\partial y} + C_2\overline{v^2}\frac{\partial \overline{w^2}}{\partial y} + 2(C_2+1)\overline{uv}\frac{\partial \overline{uv}}{\partial y}\right]\right\}$$

$$- C_1\bar{\epsilon}\left(\frac{\overline{u^2}}{\overline{q^2}} - \frac{1}{3}\right) - 4\left(\frac{2C+1}{3}\right)\overline{uv}\frac{\partial U}{\partial y} - \frac{2}{3}\bar{\epsilon}$$

$$\frac{\partial \overline{v^2}}{\partial y} = \frac{\partial}{\partial y}\left\{C_0 \frac{\overline{q^2}}{\epsilon}\left[(C_2 - \tfrac{2}{5})\overline{v^2}\frac{\partial \overline{u^2}}{\partial y} + 3(C_2 + \tfrac{3}{5})\overline{v^2}\frac{\partial \overline{v^2}}{\partial y} + (C_2 - \tfrac{2}{5})\overline{v^2}\frac{\partial \overline{w^2}}{\partial y} + 2(C_2 - \tfrac{2}{5})\overline{uv}\frac{\partial \overline{uv}}{\partial y}\right]\right\}$$

$$- C_1\bar{\epsilon}\left(\frac{\overline{v^2}}{\bar{q}^2}-\frac{1}{3}\right) - 4\left(\frac{-5C-1}{3}\right)\overline{vu}\frac{\partial U}{\partial y} - \frac{2}{3}\bar{\epsilon}$$

$$\frac{\partial \overline{w^2}}{\partial x} = \frac{\partial}{\partial y}\left\{ C_0\frac{\bar{q}^2}{\bar{\epsilon}}\left[C_2\overline{v^2}\frac{\partial \overline{w^2}}{\partial y} + 3C_2\overline{v^2}\frac{\partial \overline{v^2}}{\partial y} + (C_2+1)\overline{v^2}\frac{\partial \overline{v^2}}{\partial y} + 2C_2\overline{uv}\frac{\partial \overline{uv}}{\partial y}\right]\right\}$$

$$- C_1\bar{\epsilon}\left(\frac{\overline{w^2}}{\bar{q}^2}-\frac{1}{3}\right) - 4C\,\overline{uv}\frac{\partial U}{\partial y} - \frac{2}{3}\bar{\epsilon}$$

$$\frac{\partial \overline{uv}}{\partial x} = \overline{v^2}\frac{\partial U}{\partial y} + \frac{\partial}{\partial y}\left\{ C_0\frac{\bar{q}^2}{\bar{\epsilon}}\left[-\frac{3}{5}\overline{uv}\frac{\partial \overline{u^2}}{\partial y} + \frac{4}{5}\overline{uv}\frac{\partial \overline{v^2}}{\partial y} - \frac{1}{5}\overline{uv}\frac{\partial \overline{w^2}}{\partial y} + \frac{4}{5}\overline{v^2}\frac{\partial \overline{uv}}{\partial y}\right]\right\}$$

$$- C_1\bar{\epsilon}\frac{\overline{uv}}{\bar{q}^2} - 2\left[\frac{1}{10}\bar{q}^2 - \frac{4C+1}{3}\left(\overline{u^2}-\frac{1}{3}\bar{q}^2\right) - \frac{C-1}{3}\left(\overline{v^2}-\frac{1}{3}\bar{q}^2\right)\right]\frac{\partial U}{\partial y}$$

where $C_0 = 1/3C_1$ and $C_2 = (C_1-2)/(10+4C_1)$

Dissipation:

$$\frac{\partial \bar{\epsilon}}{\partial x} = \frac{\partial}{\partial y}\left\{ \frac{9}{70}\frac{\bar{q}^2}{\bar{\epsilon}}\left(\overline{v^2} + 2\frac{\overline{uv}^2+\overline{v^2}^2}{\bar{q}^2}\right)\frac{\partial \bar{\epsilon}}{\partial y}\right\}$$

$$- \gamma_0\frac{\bar{\epsilon}^2}{\bar{q}^2} + \gamma_1\bar{\epsilon}\frac{\overline{uv}}{\bar{q}^2}\frac{\partial U}{\partial y}$$

Appendix II

The equations in non-dimensional form for the axisymmetric wake are presented in terms of the mean velocity defect (defined as for the plane wake) and the velocity components $u = u_1/U_{1\infty}$, $v = u_2/U_{1\infty}$ and $w = u_3/U_{1\infty}$ for the axial ($x = x_1/\ell$), radial ($r = x_2/\ell$) and angular directions respectively.

Momentum equation:

$$\frac{\partial U}{\partial x} = \frac{1}{r}\frac{\partial}{\partial r}(r\,\overline{uv})$$

Reynolds stress equations:

$$\frac{\partial \overline{u^2}}{\partial x} = 2\,\overline{uv}\frac{\partial U}{\partial y} + \frac{1}{r}\frac{\partial}{\partial r}\left\{ r C_0 \frac{\overline{q^2}}{\tilde{\epsilon}}\left[(C_1+1)\overline{v^2}\frac{\partial \overline{u^2}}{\partial r} + 3C_1\overline{v^2}\frac{\partial \overline{v^2}}{\partial r} + C_1\overline{v^2}\frac{\partial \overline{w^2}}{\partial r} \right.\right.$$

$$\left.\left. + 2(C_1+1)\,\overline{uv}\frac{\partial \overline{uv}}{\partial r} + \frac{2}{r}C_1(\overline{v^2}\,\overline{w^2} - \overline{w^2}^2)\right]\right\}$$

$$- C_1\tilde{\epsilon}\left(\frac{\overline{u^2}}{\overline{q^2}} - \frac{1}{3}\right) - 1\left(\frac{2C+1}{3}\right)\overline{uv}\frac{\partial U}{\partial r} - \frac{2}{3}\tilde{\epsilon}$$

$$\frac{\partial \overline{v^2}}{\partial x} = \frac{1}{r}\frac{\partial}{\partial r}\left\{ r C_0 \frac{\overline{q^2}}{\tilde{\epsilon}}\left[(C_1 - \tfrac{2}{5})\overline{v^2}\frac{\partial \overline{u^2}}{\partial r} + 3(C_1 + \tfrac{3}{5})\overline{v^2}\frac{\partial \overline{v^2}}{\partial r} + (C_1 - \tfrac{2}{5})\overline{v^2}\frac{\partial \overline{w^2}}{\partial r} \right.\right.$$

$$\left.\left. + 2(C_1 - \tfrac{2}{5})\,\overline{uv}\frac{\partial \overline{uv}}{\partial r} + \frac{2}{r}(C_1 - \tfrac{2}{5})(\overline{v^2}\,\overline{w^2} - \overline{w^2}^2)\right]\right\}$$

$$+\frac{2}{r}C_0\frac{\bar{q}^2}{\bar{\varepsilon}}\Big[\frac{1}{5}\bar{v}^2\frac{\partial\bar{u}^2}{\partial r}+\frac{3}{5}\bar{v}^2\frac{\partial\bar{v}^2}{\partial r}-\frac{1}{5}\bar{v}^2\frac{\partial\bar{w}^2}{\partial r}$$

$$+\frac{2}{5}\overline{uv}\frac{\partial\bar{u}\bar{v}}{\partial r}-\frac{K}{5r}(\bar{v}^2\bar{w}^2-\overline{vw}^2)\Big]$$

$$-C_1\bar{\varepsilon}\left(\frac{\bar{v}^2}{\bar{q}^2}-\frac{1}{3}\right)-A\left(\frac{2C+1}{3}\right)\overline{uv}\frac{\partial U}{\partial r}-\frac{2}{3}\bar{\varepsilon}$$

$$\frac{\partial\bar{w}^2}{\partial x}=\frac{1}{r}\frac{\partial}{\partial r}\Big\{rC_0\frac{\bar{q}^2}{\bar{\varepsilon}}\Big[C_2\bar{v}^2\frac{\partial\bar{w}^2}{\partial r}+3C_2\bar{v}^2\frac{\partial\bar{v}^2}{\partial r}+(C_2+1)\bar{v}^2\frac{\partial\bar{w}^2}{\partial r}$$

$$+2C_2\overline{uv}\frac{\partial\bar{u}\bar{v}}{\partial r}+\frac{2}{r}(C_2+1)(\bar{v}^2\bar{w}^2-\overline{vw}^2)\Big]\Big\}$$

$$-\frac{2}{r}C_0\frac{\bar{q}^2}{\bar{\varepsilon}}\Big[\frac{1}{5}\bar{v}^2\frac{\partial\bar{u}^2}{\partial r}+\frac{3}{5}\bar{v}^2\frac{\partial\bar{v}^2}{\partial r}-\frac{4}{5}\bar{v}^2\frac{\partial\bar{w}^2}{\partial r}$$

$$+\frac{2}{5}\overline{uv}\frac{\partial\bar{u}\bar{v}}{\partial r}-\frac{K}{5r}(\bar{v}^2\bar{w}^2-\overline{vw}^2)\Big]$$

$$-C_1\bar{\varepsilon}\left(\frac{\bar{w}^2}{\bar{q}^2}-\frac{1}{3}\right)-4C\,\overline{uv}\frac{\partial U}{\partial r}-\frac{2}{3}\bar{\varepsilon}$$

$$\frac{\partial\bar{u}\bar{v}}{\partial x}=\bar{v}^2\frac{\partial U}{\partial r}+\frac{1}{r}\frac{\partial}{\partial r}\Big\{rC_0\frac{\bar{q}^2}{\bar{\varepsilon}}\Big[-\frac{3}{5}\overline{uv}\frac{\partial\bar{u}^2}{\partial r}+\frac{1}{5}\overline{uv}\frac{\partial\bar{v}^2}{\partial r}-\frac{1}{5}\overline{uv}\frac{\partial\bar{w}^2}{\partial r}$$

$$+\frac{K}{5}\bar{v}^2\frac{\partial\bar{u}\bar{v}}{\partial r}-\frac{2}{5r}\bar{w}^2\overline{uv}\Big]\Big\}$$

$$+\frac{1}{r}C_0\frac{\bar{q}^2}{\bar{\varepsilon}}\Big[\frac{3}{5}\overline{uv}\frac{\partial\bar{u}^2}{\partial r}+\frac{1}{5}\overline{uv}\frac{\partial\bar{v}^2}{\partial r}-\frac{4}{5}\overline{uv}\frac{\partial\bar{w}^2}{\partial r}$$

$$+\frac{2}{5}\bar{v}^2\frac{\partial\bar{u}\bar{v}}{\partial r}-\frac{K}{5r}\bar{w}^2\overline{uv}\Big]+$$

$$- C_1 \bar{\epsilon} \frac{\overline{uv}}{\bar{q}^2} - 2\left[\frac{1}{10}\bar{q}^2 - \frac{\nu C_1'}{3}(\bar{u}^2 - \tfrac{1}{3}\bar{q}^2) - \frac{e-1}{3}(\bar{v}^2 - \tfrac{1}{3}\bar{q}^2)\right]\frac{\partial U}{\partial r}$$

Dissipation:

$$\frac{\partial \bar{\epsilon}}{\partial t} = \frac{1}{r}\frac{\partial}{\partial r}\left\{\frac{q}{70}\frac{\bar{q}^2}{\bar{\epsilon}}\left(\bar{v}^2 + 2\frac{\overline{uv}^2 + \overline{v^2}^2}{\bar{q}^2}\right)\frac{\partial \bar{\epsilon}}{\partial r}\right\}$$

$$- \psi_0 \frac{\bar{\epsilon}^2}{\bar{q}^2} + \psi_1 \bar{\epsilon}\frac{\overline{uv}}{\bar{q}^2}\frac{\partial U}{\partial r}$$

PLANE WAKE CHARACTERISTICS

	$(\ell/\vartheta)\cdot[(x-x_0)/\vartheta]^{-1/2}$	$[(U_\infty - U(x,0))/U_\infty]\cdot[(x-x_0)/\vartheta]^{1/2}$	R_T
Townsend (Cylinder)	0.277	1.44	10.4
Chevray & Kovasznay (flat plate)	0.216	2.06	19.1
Calculated	0.201	2.10	20.9

ROUND WAKE CHARACTERISTICS

	$(\ell/\vartheta)\cdot[(x-x_0)/\vartheta]^{1/3}$	$[(U_\infty - U(x,0))/U_\infty]\cdot[(x-x_0)/\vartheta]^{2/3}$	R_T
Chevray (Spheroid)	0.272	2.09	23.05
Bevilaqua & Lykoudis (Sphere)	0.452	0.575	3.82
Bevilaqua & Lykoudis (Porous Disk)	0.246	2.31	28.17
Calculated	0.220	2.48	33.8

Figure Captions

Figure 1. Normalized mean velocity, plane wake.

Figure 2. Normalized streamwise energy, plane wake.

Figure 3. Normalized energy out of plane of wake.

Figure 4. Normalized cross-stream energy in plane of wake.

Figure 5. Normalized shear stress, plane wake.

Figure 6. Normalized triple correlations, plane wake.

Figure 7. Normalized mean velocity, round wake.

Figure 8. Normalized axial energy, round wake.

Figure 9. Normalized radial energy, round wake.

Figure 10 Normalized azimuthal energy, round wake.

Figure 11. Normalized shear stress, round wake.

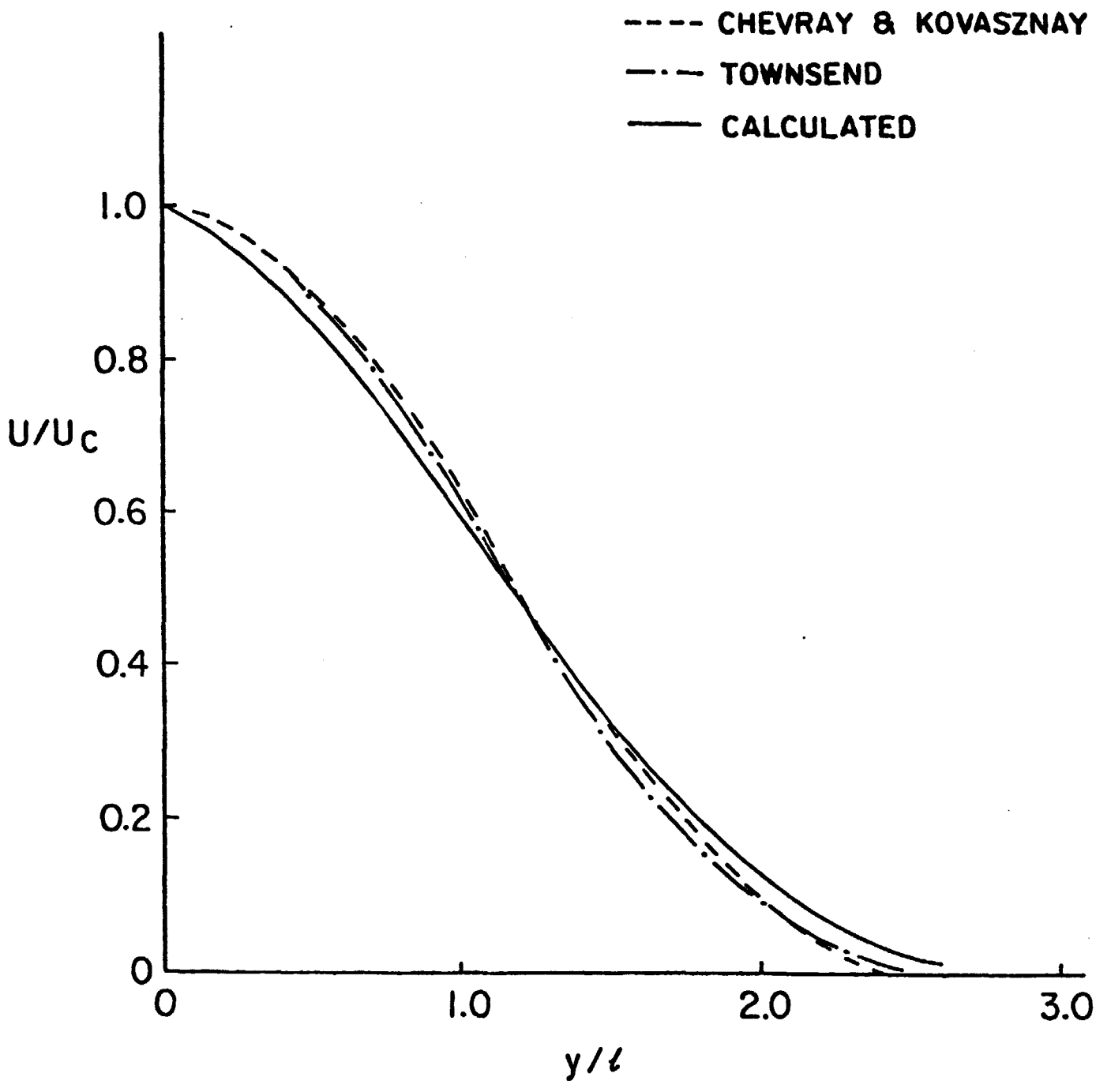

Figure 1
Rankine & Lumley.

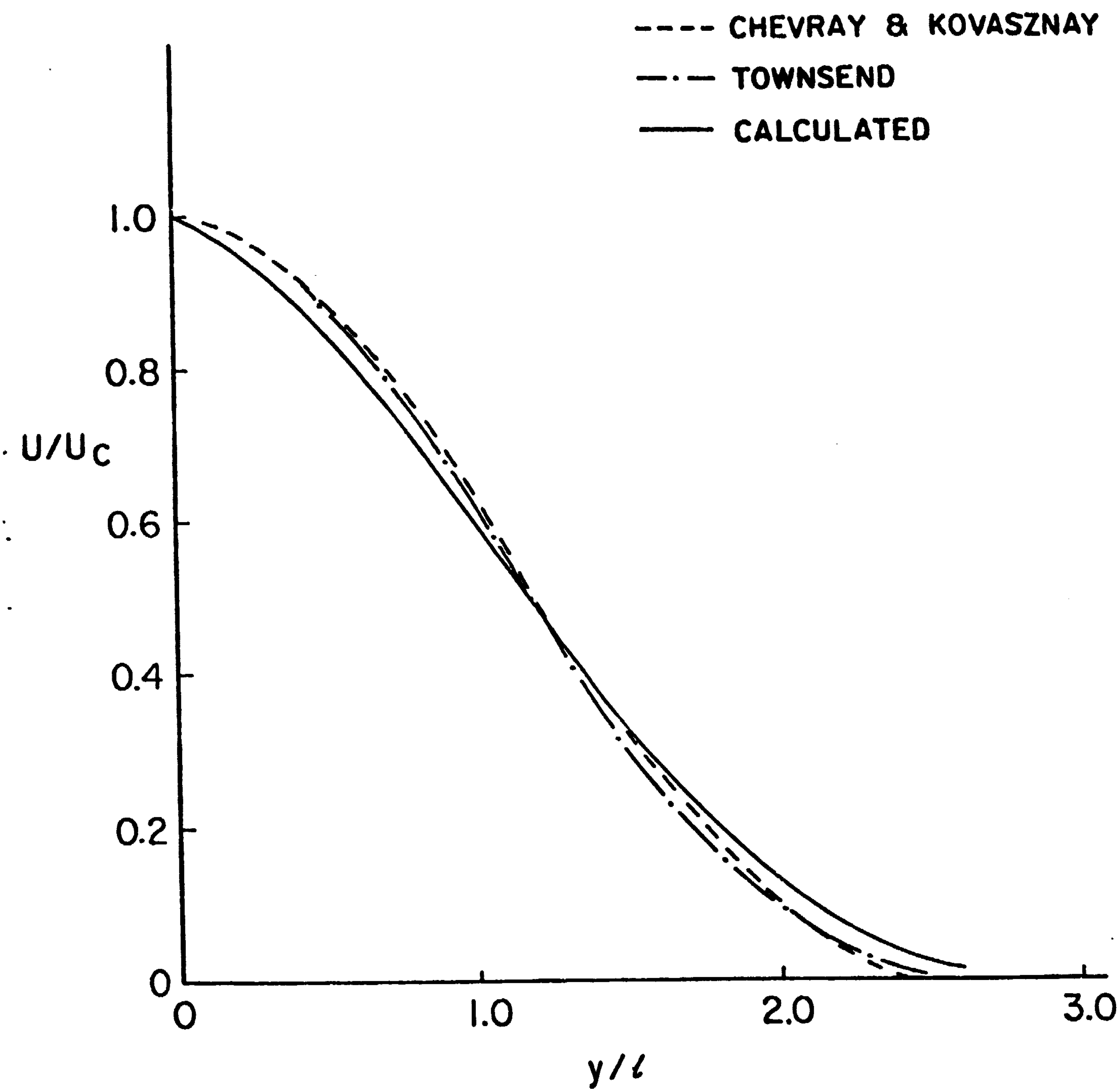

Figure 1.
Stuttee & Lumley

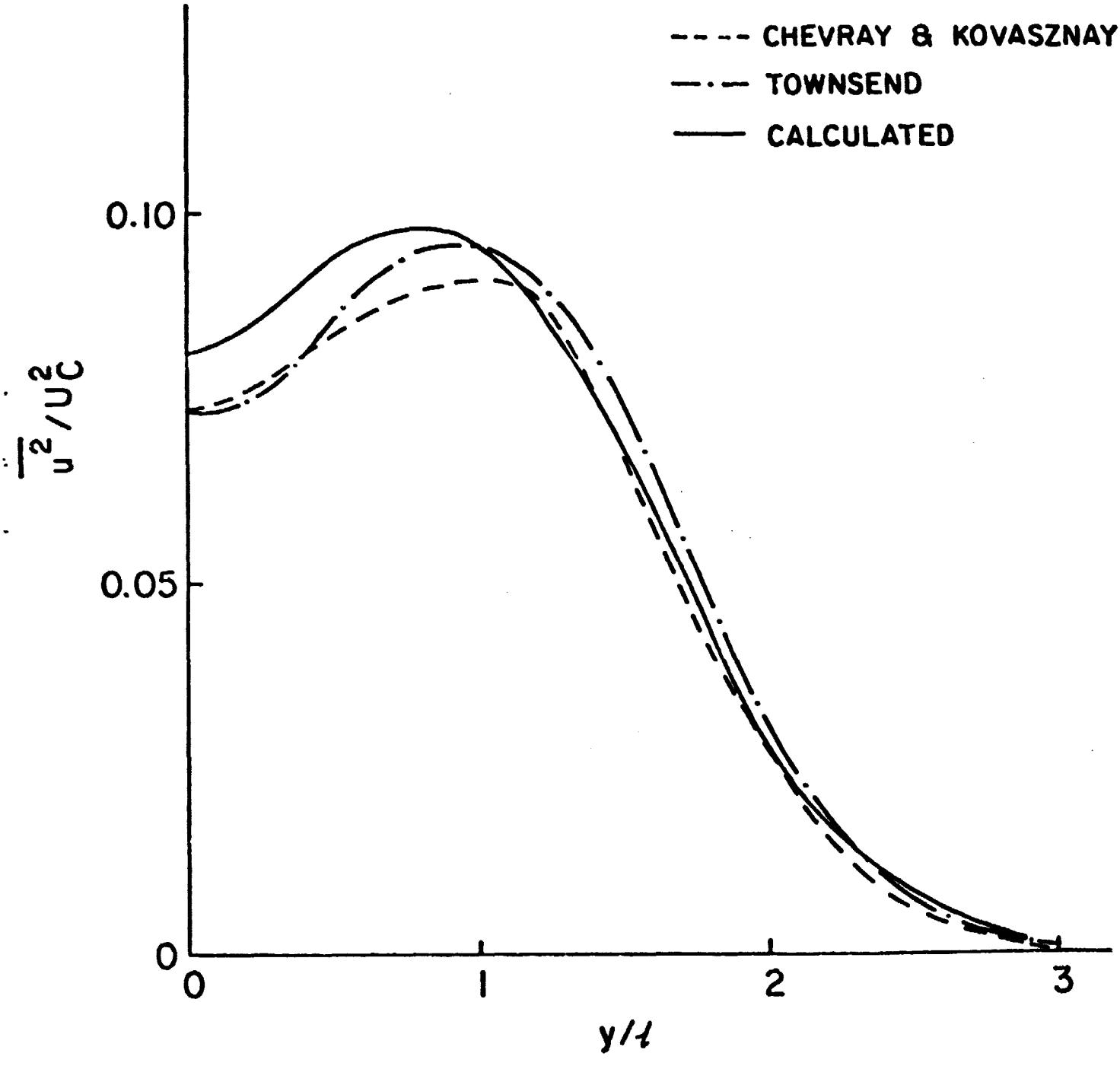

Figure 2
Transition of Turbulence

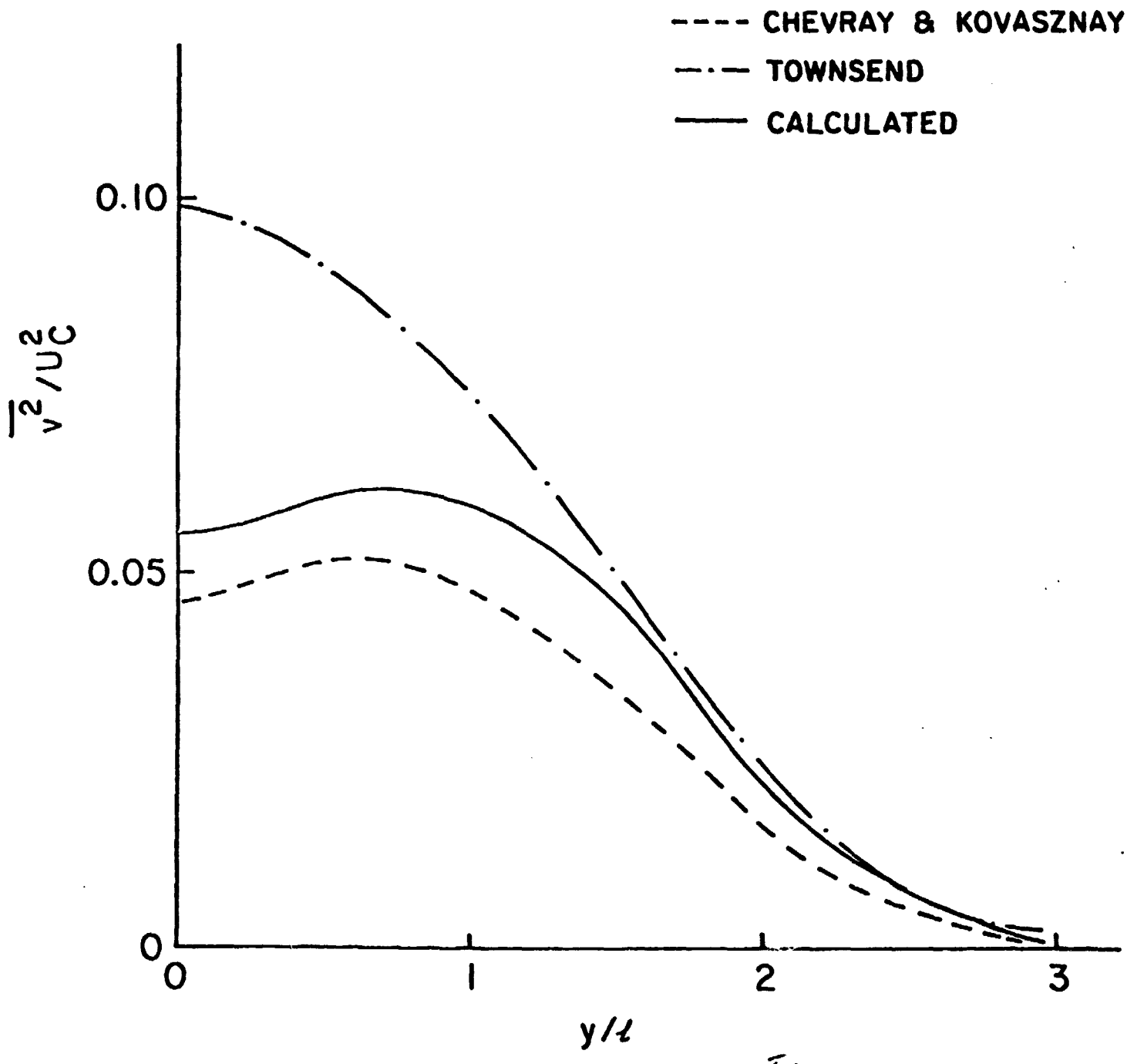

Figure 3
Townsend & Townsend

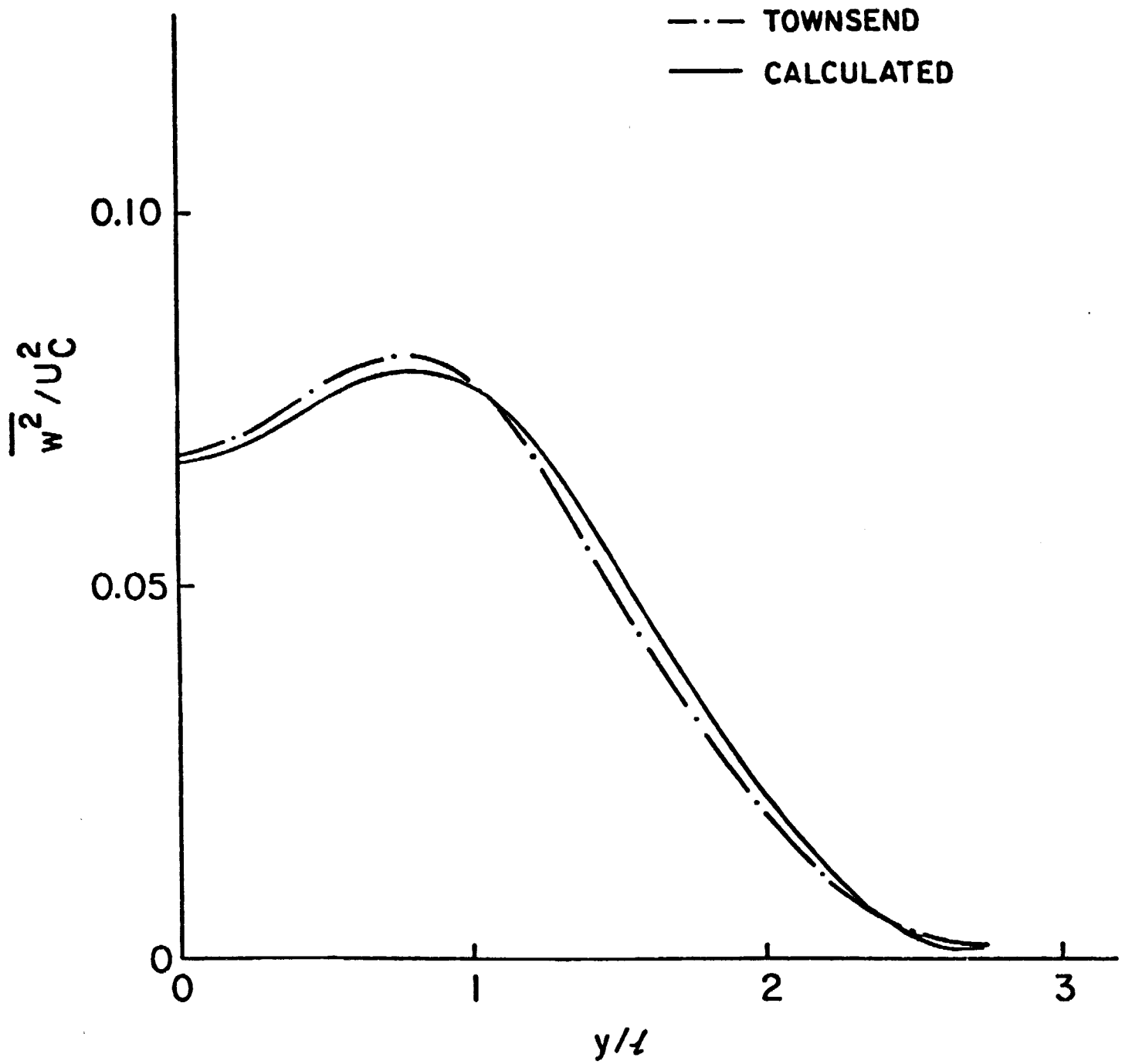

Figure 4
Townsend & Calculated

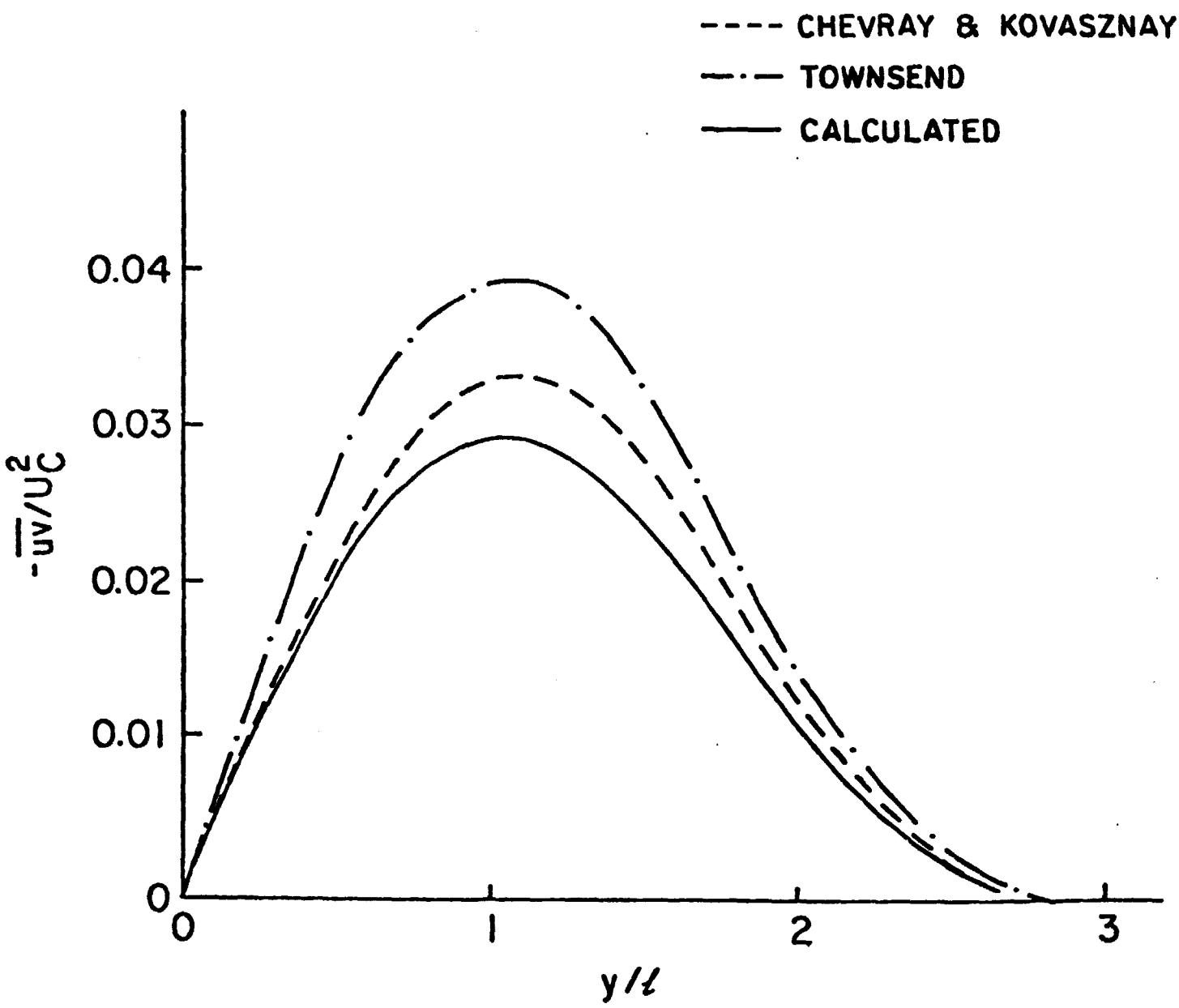

Figure 7
Townsend & Tunkey.

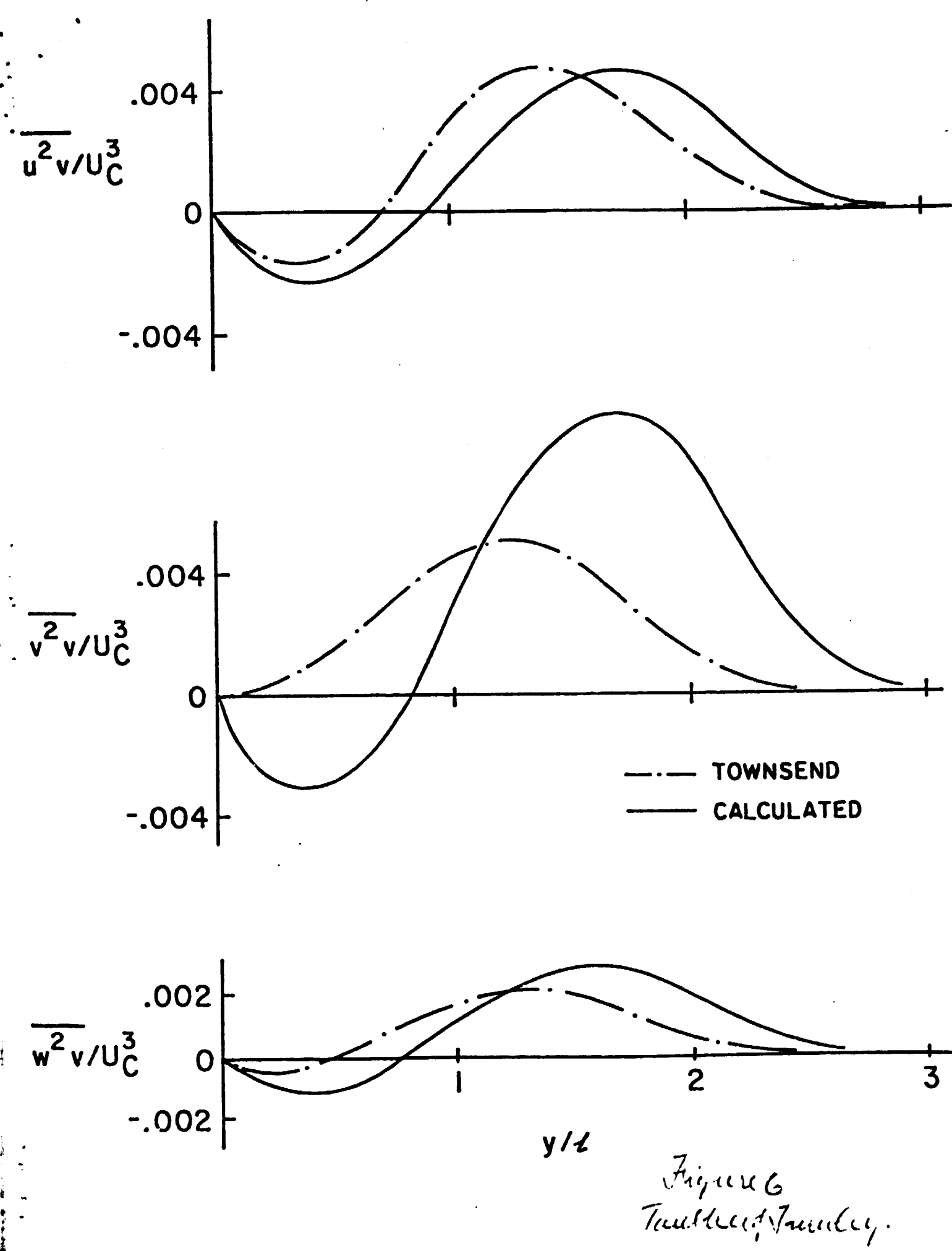

Figure 6
Townsend Tunnel.

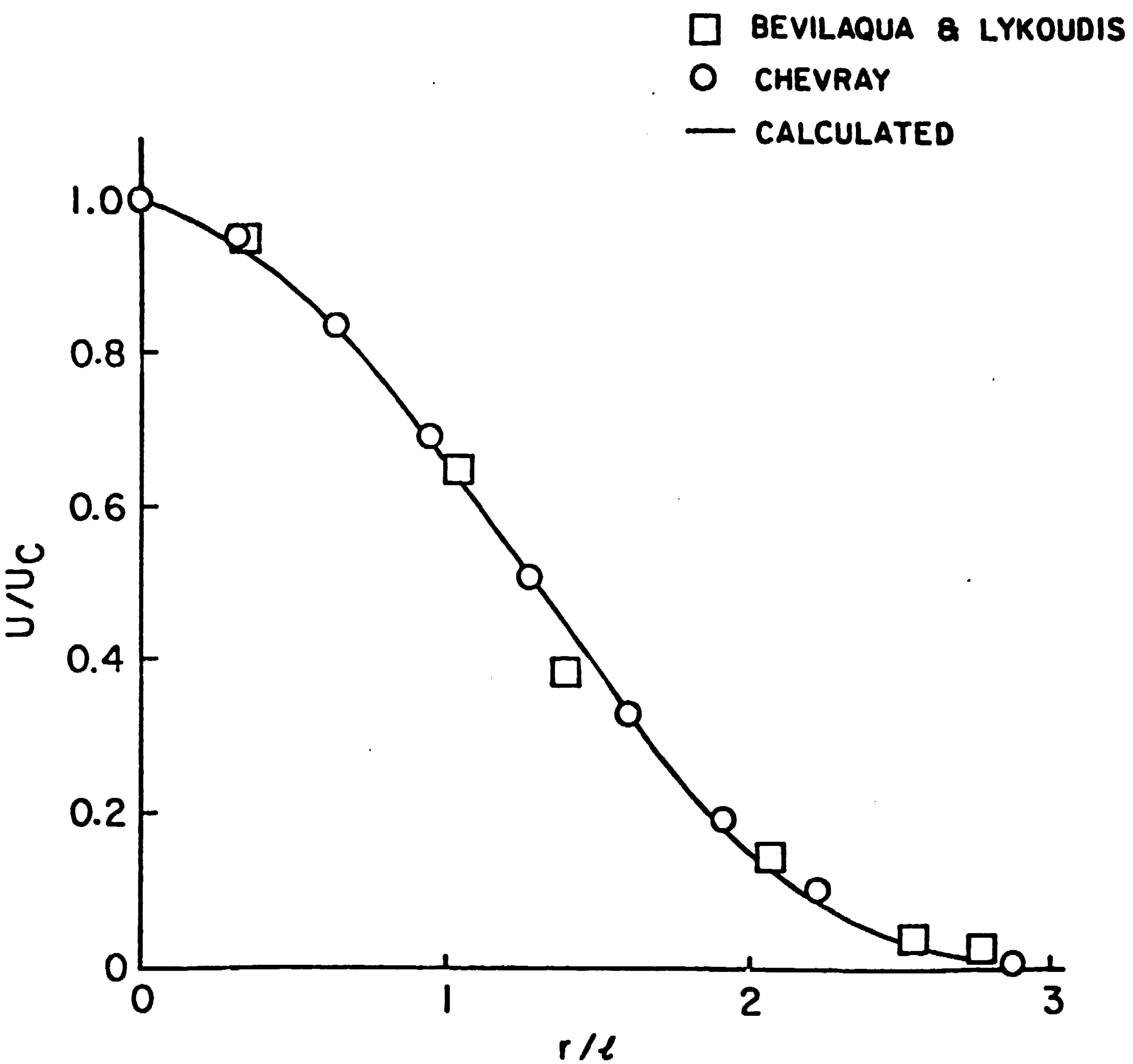

Figure 7
Tuttle & Sandry

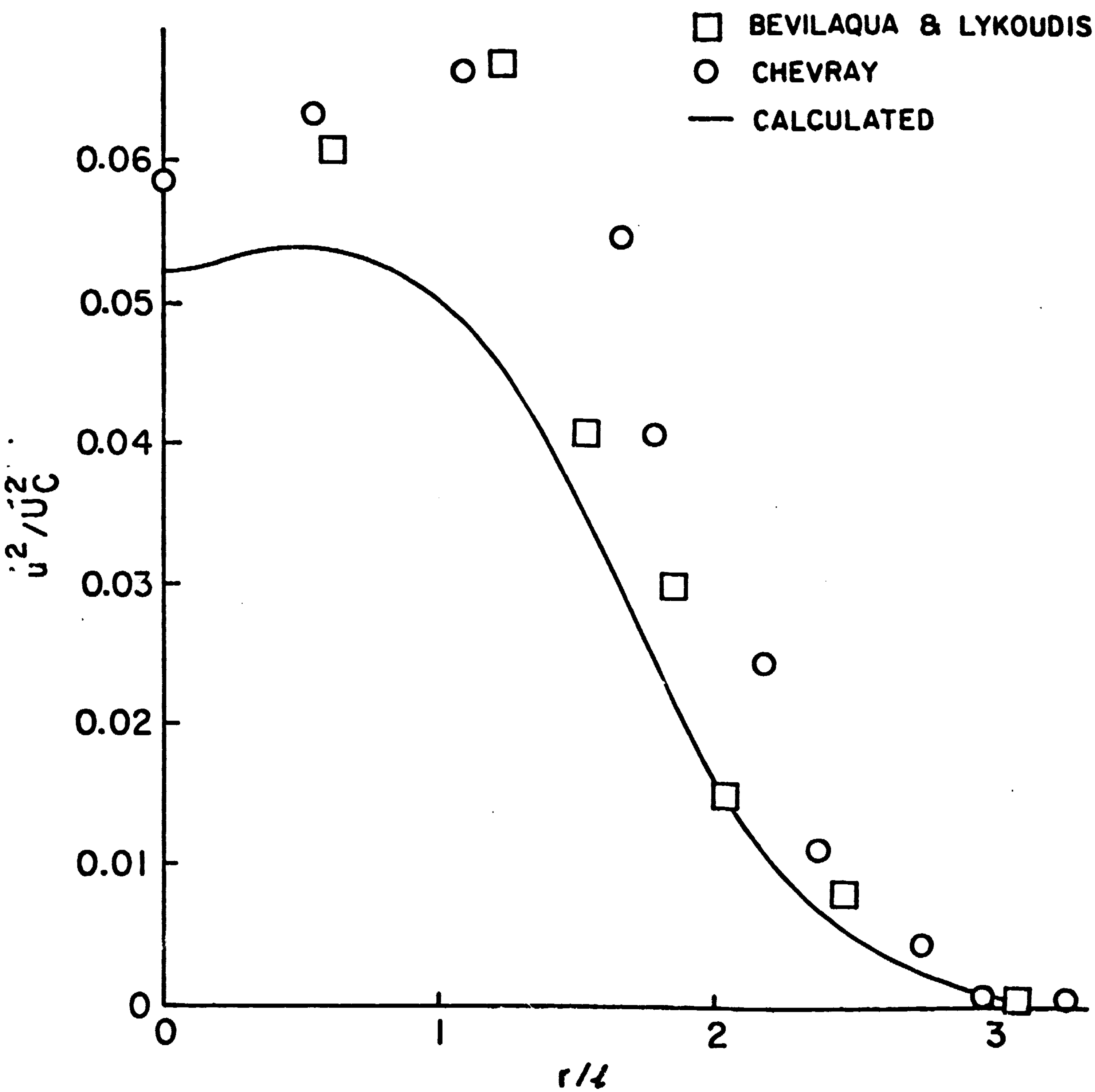

Figure 8
Tandon & Sumley

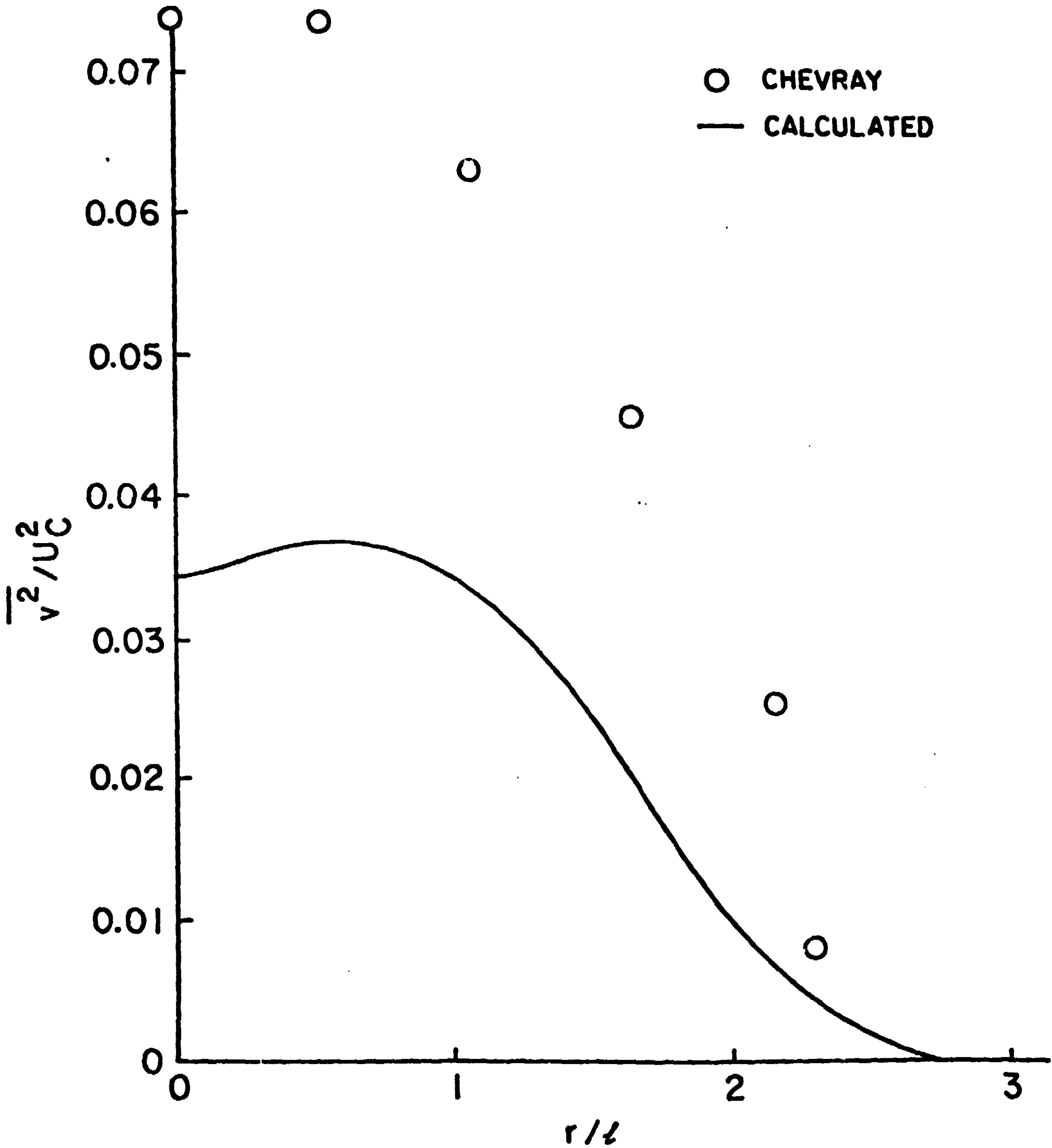

Figure 9
Taulbee & Lumley

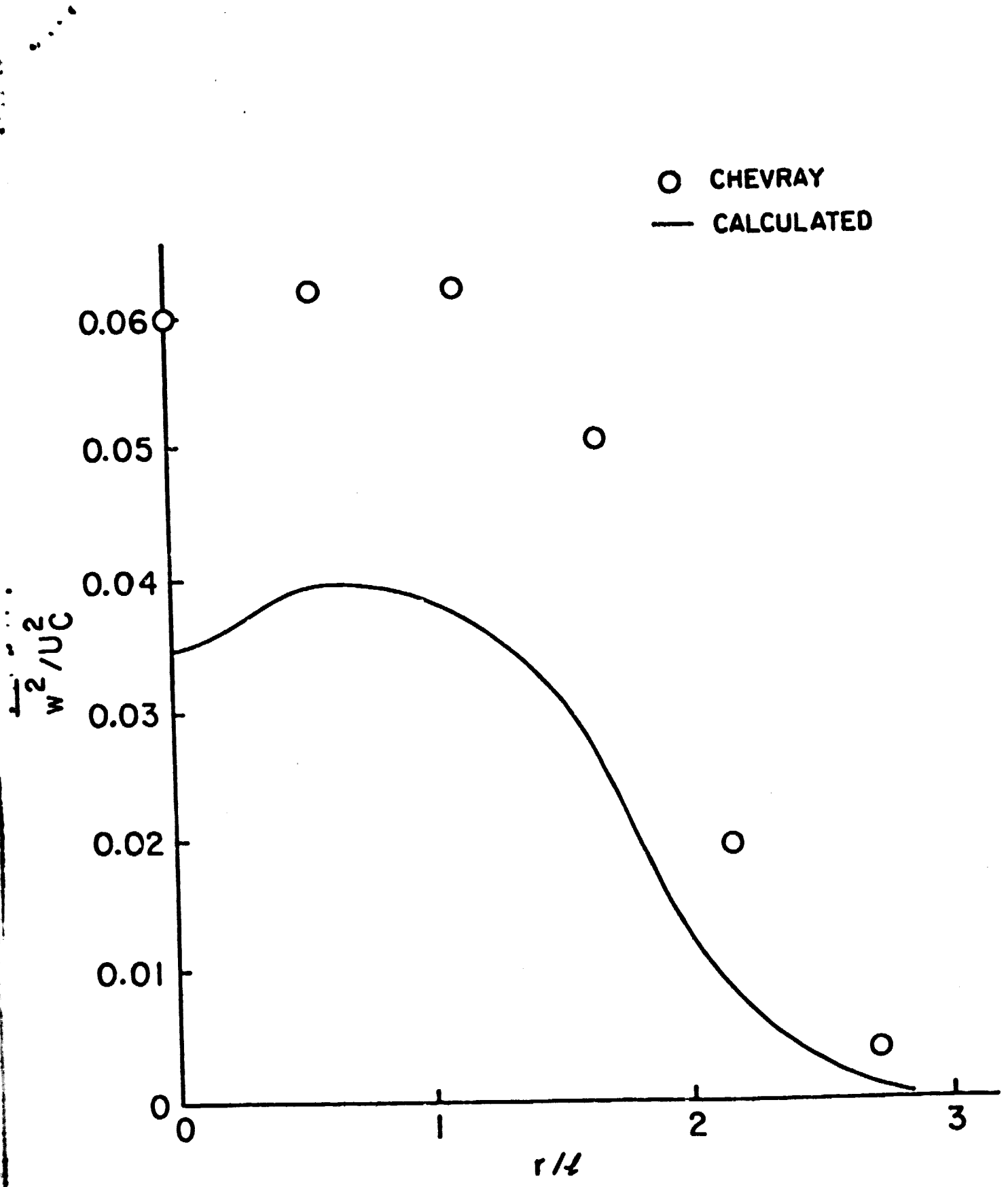

Figure 10
Fuller & Hussain

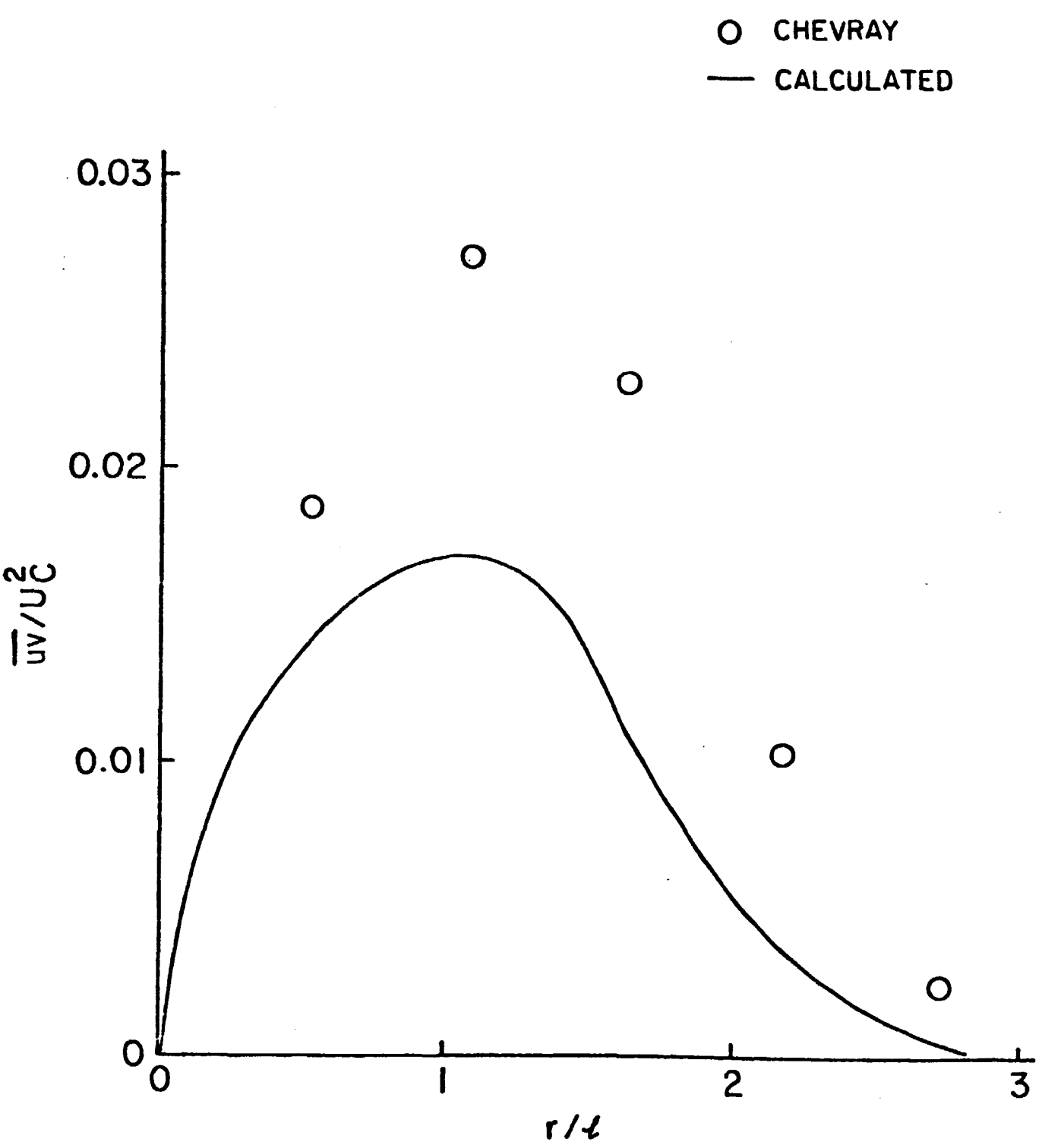

Figure 11
Trudeau & Tennekes